# Motion of Polymer Ends in Homopolymer and Heteropolymer Collapse

B. Ostrovsky and Y. Bar-Yam
Electrical, Computer and Systems Engineering Department, College of Engineering, Boston University, Boston, Massachusetts 02215 USA

ABSTRACT To investigate the polymer coil-to-globule transition we performed simulations for the kinetics of homopolymer and heteropolymer collapse. Our simulations made use of abstract models of long flexible polymers to obtain extensive statistical sampling. For a variety of these models, the simulations suggest that collapse of long polymers is dominated by diffusion of the polymer ends, which accrete monomers and small aggregates. The growth of the end aggregate was found to be nearly linear in time for homopolymers and largely unaffected by variations in microstructure. In contrast, for heteropolymers the presence of non-aggregating (hydrophilic) monomers dramatically slows and alters the growth of the end mass. In models simulated, the end mass grows roughly as the cube root of time, but still dominates aggregation along the contour. In a model where only pairwise bonding is allowed, the collapse is uniform since more flexible end motion does not result in continued end accretion. The possible significance of our results for biopolymer kinetics is discussed.

The flexible polymer coil-to-globule transition is an extensively investigated and fundamental aspect of the properties of polymers in dilute solution. Analytic arguments as well as Monte Carlo simulations have investigated the structure of various model polymers as a function of the effective temperature or relative solvent affinity through the transition ($\theta$ point). The study of model polymers is not relevant to the problem of determining the end structure in biopolymer collapse. However, the relevance of the kinetics of the coil to globule transition has increased with the development of the molten globule concept (Kuwajima, 1989; Ptitsyn, 1992). According to this picture, in its most general form, initially the polymer collapses into a compact globule which then reorganizes into a specific structure. It is the initial stage (the collapse) that may be modeled by the kinetics of the coil to globule transition. Despite the extensive investigations of the thermodynamics of the coil-to-globule transition (Lifshitz et. al., 1978; for a recent review see Chan and Dill, 1991), very little is known about the kinetics of this transition. Similar to conventional first-order transitions, nucleation may play an important role in the kinetics, whereas it plays no role at all in the thermodynamics.

A mean field kinetic theory of collapse has been developed by deGennes for homopolymer collapse during slight departures from the $\theta$ point (deGennes, 1985). Under these conditions, he suggests the polymer initially collapses into a sausage shape. Then diffusion thickens the sausage uniformly as the ends contract. As the length $N$ of the polymer increases the collapse time slows dramatically as $N^2$. This model was extended (Grosberg et al., 1988) to include the influence of topological constraints on the later stages of the collapse, with possible relevance to the molten globule rearrangements that slow the collapse further. Simulations of the kinetics of the collapse of polymer models have been limited to very short polymers (Shakhnovich et al., 1991; Miller et al., 1992). Recent simulations of longer homopolymers using more realistic models (Kavassalis and Sundararajan, 1993) are discussed below.

To develop additional insight into the kinetics of collapse, we have studied collapse in poor solvent conditions, away from the mean field regime. As long as conditions are not very close to the $\theta$ point, our results (Ostrovsky and Bar-Yam, 1994) suggest that collapse is non-uniform and proceeds rapidly by driven diffusion of the polymer ends that accrete monomers and small aggregates as they move along the contour. We have developed a scaling argument for homopolymer collapse that is independent of many details of the microstructure. In this paper we describe simulations that explore the influence of microstructure for both homopolymers and heteropolymers. We find that while the ends continue to play a special role in the collapse, certain changes in microstructure can significantly affect the scaling exponents.

Our simulations are based on abstract lattice Monte Carlo algorithms recently developed for simulating kinetics of polymers (Bar-Yam et al., 1992; Smith et al., 1992). Two different algorithms for generating the initial polymer configurations were used. In both algorithms each monomer occupies one cell of a square lattice. Polymer connectivity and excluded volume are imposed by requiring that only the nearest neighbors along the contour of a monomer reside within a prespecified bonding neighborhood. The first algorithm is unusual, but particularly efficient. In this algorithm, odd monomers and even monomers of a polymer reside in two separate spaces. Both connectivity of the polymer and excluded volume are imposed by requiring that in the opposite space only the nearest neighbors along the contour reside in the $3 \times 3 \times 3$ neighborhood of cells around each monomer. Since adjacent monomers (and only adjacent monomers) may lie on top of each other, the local polymer motion is flexible. The second algorithm is simpler to describe than the first. It makes use of one space and a $5 \times 5 \times 5$ bonding neighborhood for monomers that enables adjacent monomers to separate by one lattice site allowing flexibility in polymer dynamics. The second algorithm is similar to the bond fluctuation algorithm (Carmesin and Kremer, 1988), although

*Received for publication 10 May 1994 and in final form 27 January 1995.*
Address reprint requests to Dr. Yaneer Bar-Yam, ECS Department, 44 Cummington St., Boston University, Boston, MA 02215. Tel.: 617-353-2843; Fax: 617-353-6440; E-mail: yaneer@bu.edu.

0006-3495/95/05/1694/05 $2.00

our implementation of excluded volume differs. Among the advantages are that dynamically locked configurations do not occur (Smith et al., 1992). In both two-space and one-space algorithms, motion of monomers is performed by Monte Carlo steps that satisfy the polymer constraints.

The simulation of polymer collapse starts from a set of equilibrium polymer configurations. These configurations are generated either by local polymer Monte Carlo dynamics that satisfy dynamic scaling or by a non-local "reptation" Monte Carlo process that randomly moves monomers from one end to the other and is faster than the local Monte Carlo dynamics, but for equilibrium geometries provides equivalent results.

In simulations of collapse various scenarios for sticking are constructed whereby aggregates are formed from individual monomers. Once formed, aggregates are moved as a unit. The primary effect of hydrodynamics is included by scaling the diffusion constant of aggregates by Stokes' law for spherical bodies in $d$ dimensions $D \sim 1/M^{1/d}$. Aggregates of any size follow this diffusion law. The collapse simulations include only aggregation, and not disaggregation. This represents the behavior for collapse when the former dominates—not too close to the $\theta$ point. Since the distance from the $\theta$ point is measured using the scaling variable $N^{1/2}\Delta T$ (deGennes, 1985; Ostrovsky and Bar-Yam, 1994), the approximation becomes better for longer polymers. The scaling exponents obtained below should continue to be valid when microscopic reversibility is included. Polymer dynamics are simulated by selecting an aggregate (monomers are included as aggregates of mass 1) and moving the aggregate in one of four compass directions with a probability given by the diffusion constant and only if connectivity constraints allow—the aggregate does not leave any neighbors behind. One time interval consists of performing a number of aggregate moves equal to the number of remaining aggregates, taken to be the number at the end of the time interval. Seven different models of polymer microstructure were investigated. The first set of simulations make use of the two-space algorithm and polymers of length up to 1000 in two dimensions and 500 in three dimensions. The other models extend these results by describing variations in the microstructure and use the more physical one-space polymer algorithm for polymers of length 250 in three dimensions. The following seven paragraphs describe the different simulations.

1. In the simplest version of polymer collapse the two-space algorithm is used and collapse is simulated by eliminating the excluded volume constraint. Local Monte Carlo (diffusive) dynamics are then performed. Monomers are no longer stopped from entering the neighborhood of another monomer; however, they continue to be required not to leave any neighbors behind. This enables monomers of the same type (odd or even) to aggregate by moving on top of each other. The mass of an aggregate is set to the total number of monomers which reside on the same site. Fig. 1 shows frames from the collapse of a polymer in two dimensions. These frames illustrate the dominance of aggregation at the polymer ends as the mechanism of collapse. Some small aggregates

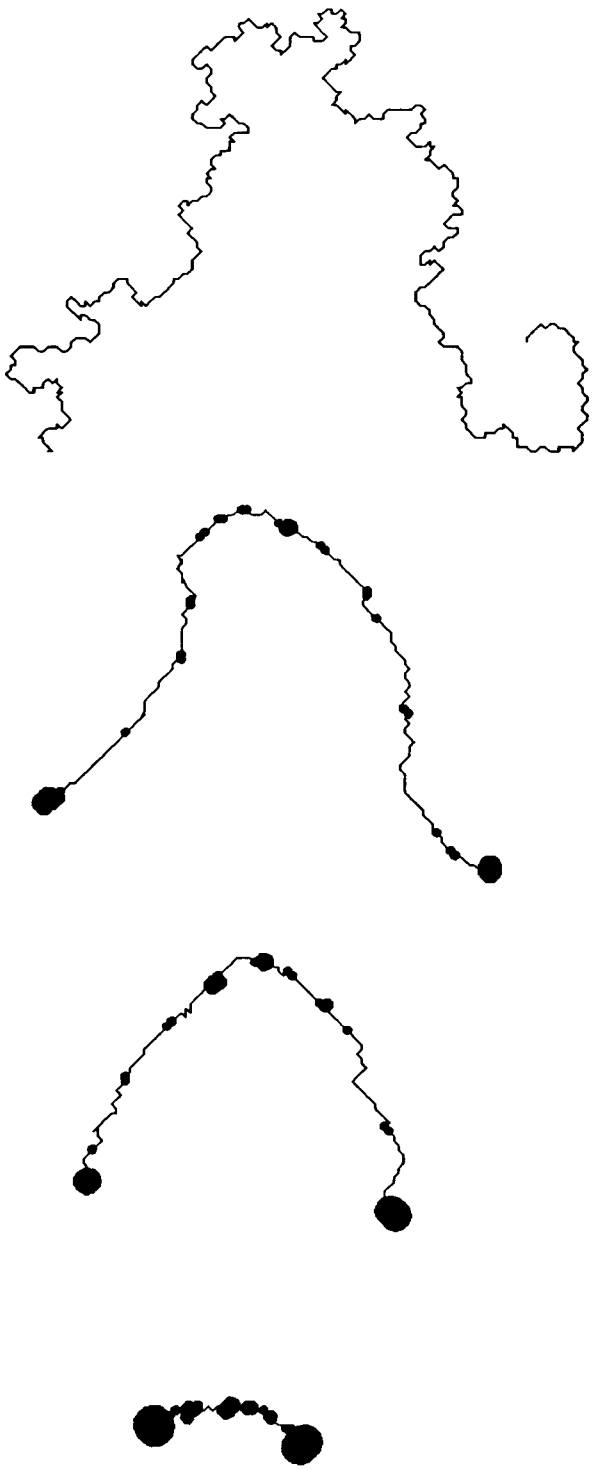

FIGURE 1 Frames "snapshots" of the collapse dynamics of a single homopolymer of length $N = 500$ monomers in two dimensions using the two-space algorithm (see text, model 1). The plot is constructed by placing dots of diameter $M^{1/2}$ for an aggregate of mass $M$. This does not reflect the excluded volume of the aggregates, which is 0 during this collapse simulation. Simulations that include excluded volume during collapse demonstrate similar results. Successive snapshots are taken at intervals of approximately 1/4 of the collapse time with the initial configuration shown at the top. The final configuration (not shown) is a single aggregate that continues to diffuse. The results demonstrate the end-dominated collapse process where the ends diffuse along the contour of the polymer accreting small aggregates.

may be seen to form along the contour of the polymer which are then accreted by the ends. The final event consists of the coalescence of the ends. Fig. 2 *a* shows the time evolution of the average mass of the polymer ends and the average mass of aggregates not including the ends for three dimensions. Longer polymers follow the collapse of the shorter polymers but extend it to longer times. This is consistent with the end dominated collapse where the length of the polymer only enters through the time at which the ends meet. The scaling follows the exponents shown in Table 1 for both two dimensions and three dimensions with exponents for the end mass $M_0$ and average mass $M$ excluding the ends:

$$M_0(t) \propto t^{s_0}; M(t) \propto t^{s} \quad (1)$$

2. The second version of collapse explores the significance of excluded volume for collapse. Since excluded volume is essential for the final structure of the polymer it might be expected to be relevant to collapse and this was completely neglected in model 1. The simulations use the more physical one-space polymer algorithm. During collapse monomers are allowed to enter the bonding neighborhood. Excluded volume is maintained during collapse by preventing monomers from occupying the same lattice site. Monomers aggregate by moving adjacent (NSEW) to other monomers. As before aggregates are moved as a unit using a step probability governed by Stokes' law. Inclusion of excluded volume increases the rate of collapse because the distance between monomers or aggregates before aggregation is reduced. Both exponents $s$ and $s_0$ increase slightly. However, we see that excluded volume does not affect overall behavior and does not dramatically change the exponents (Fig. 2 and Table 1).

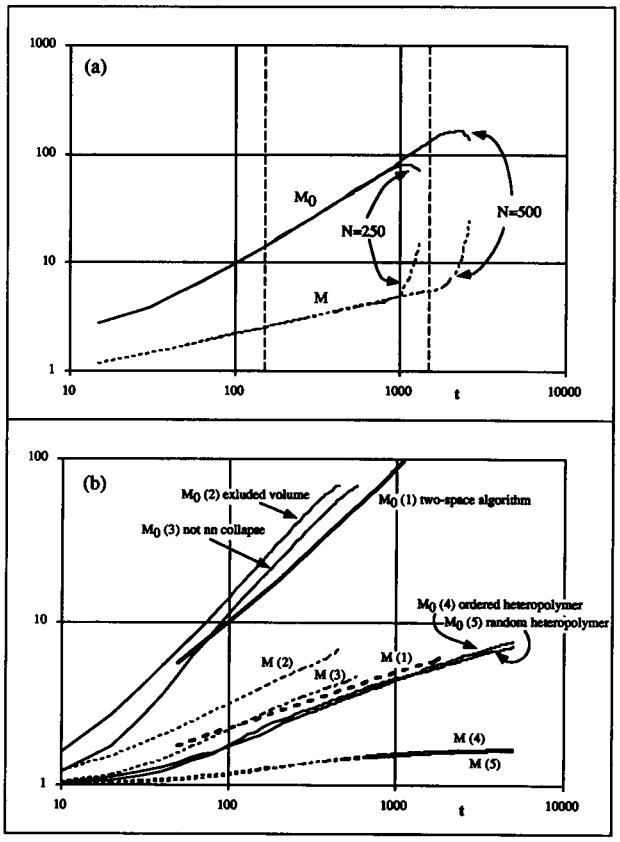


FIGURE 2 Plot of the time evolution during polymer collapse in three dimensions of the average total mass of the polymer ends $M_0(t)$ and of the average mass $M(t)$ of aggregates not including the ends. (*a*) Results of the collapse in three dimensions using the two-space algorithm and eliminating excluded volume during collapse for polymers of length $N = 500$ and $N = 250$ (500 samples). Two-dimensional results are not shown but are included in Table 1. (*b*) Scaling of five collapse models (see text for details). The end mass evolution is shown by a solid line and the mass along the contour is shown as a dashed line. (1) Repeats the scaling of (*a*) as a bold line. All other results are for polymers of length 250 (300 samples). (2) Results of one-space polymer collapse including excluded volume. (3) Same as (2) but without aggregation of neighbors along the contour. (4) Model of heteropolymer collapse using the same model as (3), however, only odd monomers collapse. (5) Similar to (4) but the monomers that collapse are selected at random from the chain.

3. One of the difficulties in models 1 and 2 is that monomers aggregate by directly attaching to their neighbor. Much of the aggregation occurs between monomers that previously were already bonded as neighbors along the chain. This would be a particularly convenient process for end aggregation and may exaggerate its importance. The aggregated structure of model 2 is formed out of rod-like structural components. A more realistic model would exclude such nearest neighbor aggregation. The third version of collapse is similar to model 2, except that nearest neighbors along the contour are prevented from aggregating to each other. Monomers or aggregates are forced to move around their nearest neighbor to bond to a monomer further along the chain. This prevents the simplest end monomer accretion of nearest neighbors. Remarkably, not only does the end-domination persist but the simulation shows (Fig. 2 and Table 1) that this does not change significantly the exponent values. Presumably this is because the need to move around neighbors to aggregate affects collapse along the contour similarly to its affect at the ends making both more difficult. The only apparent effect is an overall slowing of the collapse as seen by the shift of the $M(t)$ and $M_0(t)$ curves to longer times. The following simulations (4–7) are based on model 3.

4. The fourth version of collapse is a first model of heteropolymer collapse. Using the one-space algorithm as in model 3, only odd monomers are allowed to aggregate. This is an ordered 50% density version of a model used in studies of hydrophilic/hydrophobic collapse. Despite shielding of continued collapse by non-collapsing monomers, the collapse is still dominated by end motion for the length and time scale simulated. The overall collapse is significantly slowed; the exponent of end growth is reduced to a third of its value for the homopolymer case. There is also some indication that non-power law behavior may result in saturation of the collapse.

5. The fifth version tests the relevance of the order in model 4. The 50% aggregating monomers are selected randomly along the chain. The collapse behavior is almost the same as in model 4. Opportunistic collapse speeds the collapse at first but the scaling is slightly lower and eventually collapse is slightly slower.

**TABLE 1 Power law behavior exponents**

| Dimensions (model) | $s$ | $s_0$ | $s_0(s)$ (Eq. 3) | $s_0$-$s_0(s)$ | $x$ |
|---|---|---|---|---|---|
| 1 | 0 | 0.5 | 0.5 | 0 | 1 |
| 2 (1) | 0.154 ± 0.001 | 0.773 ± 0.001 | 0.769 ± 0.001 | 0.004 ± 0.001 (0.5%) | 0.493 ± 0.002 |
| 3 (1) | 0.337 ± 0.002 | 0.982 ± 0.005 | 1.003 ± 0.002 | −0.021 ± 0.005 (2%) | 0.362 ± 0.007 |
| 3 (2) | 0.484 ± 0.002 | 1.102 ± 0.004 | 1.113 ± 0.002 | −0.011 ± 0.004 (1%) | 0.346 ± 0.006 |
| 3 (3) | 0.453 ± 0.002 | 1.079 ± 0.004 | 1.090 ± 0.002 | −0.011 ± 0.004 (1%) | 0.347 ± 0.006 |
| 3 (4) | 0.061 ± 0.001 | 0.363 ± 0.001 | 0.796 ± 0.001 | | 1.92 ± 0.002 |
| 3 (5) | 0.050 ± 0.001 | 0.293 ± 0.001 | 0.787 ± 0.001 | | 2.58 ± 0.002 |

Power law behavior exponents are defined in the text (Eq. 1) and fitted to the simulation results of Fig. 2. Fits were chosen to minimize standard errors. Errors given are only statistical. Results are compared to the scaling relation given by Eq. 3. An effective diffusion constant scaling exponent $x$ is indicated in the last column. For the first five rows $x$ may be compared with unmodified Stokes' law $x = 1/d$. One-dimensional results are included for comparison and are exact.

6. The sixth version of collapse uses the one-space algorithm of model 3; however, collapse only includes pairwise bonding. Once two monomers are bonded, other monomers that become adjacent are not aggregated. End dominance in this case would correspond to a progressive pairing from the ends inward. A plot of the pair-density along the chain (Fig. 3 *a*) shows that, despite a tendency toward more rapid pairing at the ends, the collapse is essentially uniform.

7. The seventh version is a second model for heteropolymer collapse (Fig. 3 *b*) where pairwise bonding is allowed as in model 6; however, only even-odd monomer combinations are allowed for pairwise bonding. The results do not differ significantly from model 6.

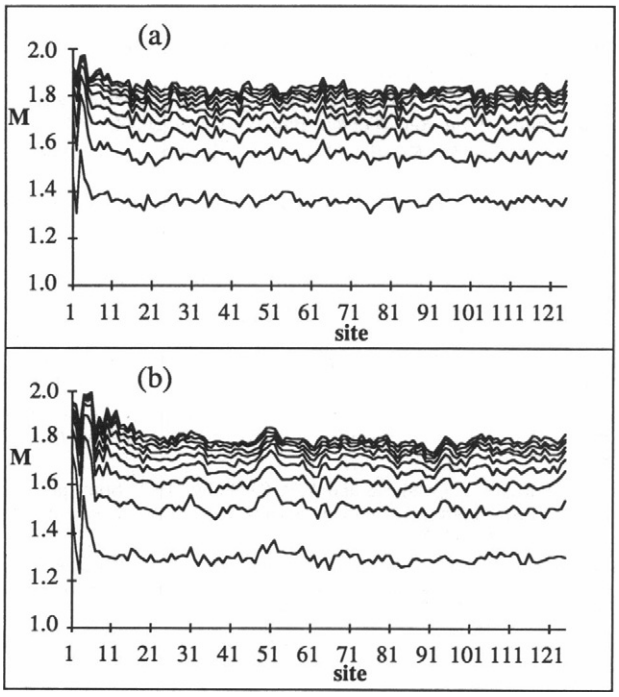


FIGURE 3 Plots of the average aggregate mass at every site along the contour when collapse only allows pairwise bonding. Collapse is uniform except for a tendency for the monomers near the end to pair-up first. The minimum mass is 1 and the maximum mass is 2. The collapsing polymer has a length $N = 250$. By symmetry only the first 125 sites are shown. (*a*) Case 6 of arbitrary monomer bonding with the exception of no nearest neighbor bonding. (*b*) Case 7 of only odd-to-even monomer bonding. Progressively later times are shown separated by 50 updates (*a*) and 100 updates (*b*). For clarity only the first 10 lines are shown.

A more complete discussion of the results of our simulations of homopolymer and heteropolymer collapse can be based on a scaling argument for collapse that includes the possibility of preferential end mass accretion (Ostrovsky and Bar-Yam, 1994). We review this argument briefly and discuss its relevance to the simulations. Every time step the end aggregate with mass $M_0(t)$ has a probability proportional to its diffusion constant of growing by accreting an aggregate nearby along the chain, assumed to be a distance $d_0$ away with an average mass $M(t)$. This holds independent of many microscopic details, such as whether or not excluded volume is maintained. It also holds when aggregation is reversible but the process is slowed down by the reverse reactions. It would not apply if the probability of disaggregation grew with the size of the aggregate, resulting in a limiting size of the aggregate and incomplete collapse of the polymer. Thus $M_0(t)$ satisfies

$$\frac{dM_0(t)}{dt} = \lambda(\Delta T/\theta)\, M(t) D_0(t)/d_0^2 \qquad (2)$$

where $\lambda(\Delta T/\theta)$ is a factor accounting for degree of reversibility (proximity to the $\theta$ point). By Stokes' law $D_0(t) = 1/M_0(t)^{1/d}$ is the diffusion constant of the end aggregate at time $t$. Assuming scaling (Eq. 1) we obtain:

$$s_0 = (s + 1)d/(d + 1) \qquad (3)$$

For $s < d$, $s_0 > s$ and the growth of the ends is faster than the growth of the width of the chain and end collapse dominates for long enough polymers. If scaling continues to be valid this expression can be generalized to include a variety of additional local kinetic effects such as the screening of the end aggregate by non-accreting monomers (e.g., hydrophilic monomers) by writing

$$\frac{dM_0(t)}{dt} = \lambda(\Delta T/\theta)\, M(t) f(t) D_0(t)/d_0^2 \qquad (2')$$

where $f(t) = 1/M_0(t)^c$. This would be equivalent to replacing Stokes' law by a different exponent $D_0(t) = 1/M_0(t)^x$ where $x = c + 1/d$. The generalization of Eq. 3 is

$$s_0 = (s + 1)/(x + 1) \qquad (3')$$

In Table 1 values of the scaling exponent from the simulations described here are compared with the scaling relation result and are in close agreement with a small but possibly

non-zero deviation for cases 1–3. The agreement with the scaling relationship is striking, since there are corrections which may be expected due to the neglect of changes in both curvature and compression of the polymer at the ends. However, the scaling relation of Eq. 3 breaks down for the case of heteropolymer collapse where the presence of hydrophilic monomers prevents aggregation in a way that changes with the size of the aggregate. We have indicated in Table 1 the value of $x$ which would be required for Eq. 3′ to hold.

The time of collapse in end-dominated collapse can be estimated from the time that it takes until the ends consume the whole polymer,

$$N \sim \tau^{s_0}$$

so the scaling of the collapse time follows

$$\tau \sim N^{1/s_0}.$$

This is the time until the ends meet in the middle. For homopolymer collapse $1/s_0 = 1.018 \pm 0.005(1)$, $0.907 \pm 0.003(2)$, $0.927 \pm 0.003(3)$ in three dimensions (errors are statistical). Thus the collapse time scales approximately linearly with polymer length in three dimensions. The maximum values allowed by the scaling relations for $x = 1/d$ are 3/2 in two dimensions and 4/3 in three dimensions. These values (even the upper limits) are significantly smaller than the uniform collapse exponent of 2. This should be contrasted with the model heteropolymer collapse that scales as $1/s_0 = 2.75 \pm 0.007(4)$ and $3.41 \pm 0.008(5)$. The regime of applicability of the different scaling exponents will have significance for the time scale of long biopolymer collapse.

There exist both simulations and experimental results that suggest that end-dominated collapse can be expected to apply under more realistic circumstances than the abstract polymer simulations reported here. However, these investigations did not obtain accurate scaling exponents that can be compared with the present results.

Molecular dynamics simulation of polyethylene crystallization (Kavassalis and Sundararajan, 1993) performed using conventional potentials for 1000 monomers found that for high temperature (600 K) or without a torsional potential the collapse displays pictures qualitatively similar to Fig. 1 for individual collapses. We note that these simulations include reversibility and use molecular dynamics rather than the Monte Carlo described here. With the torsional potential at 300 K, the stiffness of the polymer results in too few persistence lengths. Statistics for many collapses are not available but for a few collapses the scaling of collapse time with polymer length at 600 K appears to be linear, consistent with our results for homopolymer collapse.

There are few existing experiments that address the very initial stages of the collapse kinetics. The collapse of a single DNA filament has been observed by fluorescence microscopy. The images taken show that collapse was initiated at an end and occurred by a process analogous to "rolling up a ball of string" (Fig. 6 in Bustamante, 1991). These observations show driven diffusion end motion consistent with our results. In addition they suggest that a nonlinear polymer stiffness can lead to a wait time before the end can initiate (nucleate) the collapse. This property of polymer microstructure will be explored in future simulations.

Finally, recent investigations of proteins whose ends have been modified (Flanagan et al., 1993) show dramatic structural changes. It may be possible to make use of end-modified polymers to study the importance of ends in collapse kinetics. Our results suggest that in the early stages of folding some secondary structure formation should occur analogous to local aggregation along the chain. The end motion should primarily affect the early selection of longer range tertiary contacts. However, we expect that the longer time scale for the initial stages of DNA collapse should enable more detailed tests.

We thank A. Yu. Grosberg, R. C. Davenport, Jr., C. DeLisi, D. M. Engelman, V. A. Bloomfield, and C. Bustamante for helpful discussions, and M. A. Smith for contributions to the simulations.

## REFERENCES

Bar-Yam, Y., Y. Rabin, and M. A. Smith. 1992. Parallel processing simulation of polymers. *Macromol. Rep.* 25:2985–2986.

Bustamante, C. 1991. Direct observation and manipulation of single DNA molecules using fluorescence microscopy. *Annu. Rev. Biophys. Biophys. Chem.* 20:415–446.

Carmesin I., and K. Kremer. 1988. The bond fluctuation method: a new effective algorithm for the dynamics of polymers in all spatial dimensions. *Macromolecules.* 21:2819–2823.

Chan, H. S., and K. A. Dill. 1991. Polymer principles in protein structure and stability. *Annu. Rev. Biophys. Biophys. Chem.* 20:447–490.

deGennes, P. G. 1985. Kinetic collapse for a flexible coil. *J. Phys. Lett.* 46:L639–642.

Flanagan, J. M., M. Kataoka, T. Fujisawa, and D. M. Engelman. 1993. Mutations can cause large changes in the conformation of a denatured protein. *Biochemistry.* 32:10359–10370.

Grosberg, A. Y., S. K. Nechaev, and E. I. Shakhnovich. 1988. The role of topological constraints in the kinetics of collapse of macromolecules. *J. Phys. France.* 49:2095.

Kavassalis, T. A., and P. R. Sundararajan. 1993. A molecular dynamics study of polyethylene crystallization. *Macromolecules.* 26:4144–4150.

Kuwajima, K. 1989. The molten globule state as a clue for understanding the folding and cooperativity of globular-protein structure. *Proteins.* 6:87–103.

Lifshitz, I. M., A. Y. Grosberg, and A. R. Khokhlov. 1978. Some problems of the statistical physics of polymer chains with volume interaction. *Rev. Mod. Phys.* 50:683–713.

Miller, R., C. A. Danko, M. J. Fasolka, A. C. Balazs, H. S. Chan, and K. A. Dill. 1992. Folding kinetics of proteins and copolymers. *J. Chem. Phys.* 96:768–780.

Ostrovsky, B., and Y. Bar-Yam. 1994. Irreversible polymer collapse in 2 and 3 dimensions. *Europhys. Lett.* 25:409–414.

Ptitsyn, O. B. 1992. The molten globule state. *In* Protein Folding. T. E. Creighton, editor. W. H. Freeman, New York. 243–300.

Shakhnovich, E., G. Farztdinov, A. M. Gutin, and M. Karplus. 1991. Protein folding bottlenecks: a lattice Monte-Carlo simulation. *Phys. Rev. Lett.* 67:1665–1668.

Smith, M. A., Y. Bar-Yam, B. Ostrovsky, Y. Rabin, C. H. Bennett, N. Margolus, and T. Toffoli. 1992. Parallel processing simulation of polymers. *J. Comp. Polymer Sci.* 2:165–171.